DOI:10.1158/1078-0432.CCR-10-3349

Clinical Cancer Research

BRAF Activation Induces Transformation and Then Senescence in Human Neural Stem Cells: A Pilocytic Astrocytoma Model

Eric H. Raabe, Kah Suan Lim, Julia M. Kim, et al.

Clin Cancer Res 2011;17:3590-3599. Published online June 1, 2011.

DOI:10.1158/1078-0432.CCR-10-3349

Human Cancer Biology

Clinical Cancer Research

BRAF Activation Induces Transformation and Then Senescence in Human Neural Stem Cells: A Pilocytic Astrocytoma Model

Eric H. Raabe[1], Kah Suan Lim[2], Julia M. Kim[3], Alan Meeker[2], Xing-gang Mao[2], Guido Nikkhah[4], Jarek Maciaczyk[5], Ulf Kahlert[4], Deepali Jain[2], Eli Bar[2], Kenneth J. Cohen[1], and Charles G. Eberhart[2]

Abstract

Purpose: BRAF is frequently activated by gene fusion or point mutation in pilocytic astrocytoma, the most common pediatric brain tumor. We investigated the functional effect of constitutive BRAF activation in normal human neural stem and progenitor cells to determine its role in tumor induction in the brain.

Experimental Design: The constitutively active $BRAF^{V600E}$ allele was introduced into human neurospheres, and its effects on MAPK (mitogen-activated protein kinase) signaling, proliferation, soft agarose colony formation, stem cell phenotype, and induction of cellular senescence were assayed. Immunohistochemistry was used to examine $p16^{INK4a}$ levels in pilocytic astrocytoma.

Results: $BRAF^{V600E}$ expression initially strongly promoted colony formation but did not lead to significantly increased proliferation. $BRAF^{V600E}$-expressing cells subsequently stopped proliferating and induced markers of oncogene-induced senescence including acidic β-galactosidase, PAI-1, and $p16^{INK4a}$ whereas controls did not. Onset of senescence was associated with decreased expression of neural stem cell markers including SOX2. Primary pilocytic astrocytoma cultures also showed induction of acidic β-galactosidase activity. Immunohistochemical examination of 66 pilocytic astrocytomas revealed $p16^{INK4a}$ immunoreactivity in the majority of cases, but patients with tumors negative for $p16^{INK4a}$ had significantly shorter overall survival.

Conclusions: BRAF activation in human neural stem and progenitor cells initially promotes clonogenic growth in soft agarose, suggesting partial cellular transformation, but oncogene-induced senescence subsequently limits proliferation. Induction of senescence by BRAF may help explain the low-grade pathobiology of pilocytic astrocytoma, whereas worse clinical outcomes associated with tumors lacking $p16^{INK4a}$ expression could reflect failure to induce senescence or an escape from oncogene-induced senescence. *Clin Cancer Res; 17(11); 3590–9. ©2011 AACR.*

Introduction

Pilocytic astrocytoma is the most common childhood brain tumor (1). It often follows an indolent course, with waxing and waning growth kinetics, and some cases of spontaneous regression have been reported (2, 3). Tumors frequently respond to treatment with chemotherapy or radiation therapy, but they can regrow after a period of quiescence, requiring further therapy (2, 4). Several laboratories have identified constitutive activation of the RAS/RAF pathway as the primary molecular alteration in pilocytic astrocytoma (5–11). The most common alteration is a tandem duplication at chromosome 7q34 involving *BRAF*, an upstream regulator of the MAPK (mitogen-activated protein kinase) pathway. In most cases, the regulatory domain of *BRAF* is lost, and the catalytic domain is fused to KIAA1549, causing constitutive activation of downstream signaling, as measured by extracellular-signal regulated kinase (ERK) activation (8, 12). A subset of pilocytic astrocytoma lacking the KIAA1549:BRAF fusion instead contain mutations at *BRAF* codon 600, resulting in a single amino acid substitution ($BRAF^{V600E}$) that also constitutively activates the kinase (6, 7, 9, 10, 12, 13). Finally, point mutations in *KRAS*, fusions involving *RAF1* or small insertions activating *BRAF*, have been identified in rare cases (5, 7, 11, 14).

Activation of BRAF in melanocytic nevi and melanoma has been associated with a process known as "oncogene-induced senescence," in which an inciting oncogenic stimulus also limits neoplastic growth via induction of cellular senescence (15). The mechanisms by which BRAF

Authors' Affiliations: [1]Division of Pediatric Oncology and Departments of [2]Pathology and [3]Pediatrics and Adolescent Medicine, Johns Hopkins University School of Medicine, Baltimore, Maryland; and Departments of [4]Stereotactic and Functional Neurosurgery and [5]General Neurosurgery, Neurocenter, University Hospital Freiburg, Freiburg, Germany

Note: Supplementary data for this article are available at Clinical Cancer Research Online (http://clincancerres.aacrjournals.org/).

Corresponding Author: Charles G. Eberhart, Department of Pathology, Johns Hopkins University School of Medicine, 720 Rutland Ave, Ross Bldg 558, Baltimore, MD 21205. Phone: 410-502-5157; Fax: 410-955-0028; E-mail: ceberha@jhmi.edu or Eric H. Raabe, Division of Pediatric Oncology, Johns Hopkins University School of Medicine, 720 Rutland Ave, Ross Bldg 558, Baltimore, MD 21205. E-mail: eraabe2@jhmi.edu

doi: 10.1158/1078-0432.CCR-10-3349

DOI:10.1158/1078-0432.CCR-10-3349

Translational Relevance

BRAF and the MAPK (mitogen-activated protein kinase) signaling cascade are active in the majority of pilocytic astrocytoma, but the oncogenic effects of these hallmark molecular changes are poorly understood. Using neurospheres derived from normal human fetal cortex, we found that early increases in anchorage-independent growth after BRAF activation were followed by proliferation arrest and induction of cellular senescence. We also detected the senescence markers acidic β-galactosidase and p16INK4a in pilocytic astrocytoma samples. Patients whose tumors lacked $p16^{INK4a}$ protein had significantly shorter survival. Immunohistochemical analysis of $p16^{INK4a}$ may therefore aid in therapeutic stratification. The findings presented here suggest that the indolent growth of pilocytic astrocytoma may be due to oncogene-induced senescence, similar to what is observed in melanocytic nevi. Failure to induce senescence, or an escape of the tumor from senescence, may result in more aggressive tumor biology. Understanding the regulation of oncogene-induced senescence may help develop more effective treatments of pediatric low-grade gliomas.

activation leads to transformation of neural cells into pilocytic astrocytomas are not yet clear, but their often indolent growth pattern suggests that oncogene-induced senescence may play a role. To address this, we used human neural stem and progenitor cells isolated from first trimester fetal autopsy specimens and grown in long-term culture (16, 17) to examine the effects of BRAF activation on cells from which pilocytic astrocytoma are thought to arise (18). We found that expression of $BRAF^{V600E}$ in neurospheres derived from cerebral cortex initially promoted colony formation in soft agar, but the cells subsequently became senescent, with increased expression of acidic β-galactosidase, PAI-1 and $p16^{INK4a}$. This suggests that growth of pilocytic astrocytoma may be regulated in part by the induction of senescence.

Materials and Methods

Neurosphere cell culture

Cells were obtained from first trimester human fetal autopsy specimens in concordance with German law and Ethics Board evaluation. The study was also approved by the Johns Hopkins Institutional Review Board. Cells from cerebral cortex were microdissected and processed as described previously (19) and then passaged in neurosphere media [30% Ham's F12 medium, 70% DMEM, 5% B27 reagent (Invitrogen), 1% L-glutamine, 1% antibiotic-antimycotic, 5 μg/mL heparin, 20 ng/mL fibroblast growth factor (FGF), and 20 ng/mL endothelial growth factor (EGF)]. Cells were split at high density after incubation with Accutase (Sigma–Aldrich) and gentle trituration.

DNA constructs and viral infection

The construct encoding $BRAF^{V600E}$ was purchased from Addgene (Addgene plasmid 15269; ref. 20). The $BRAF^{V600E}$ cDNA was subcloned into the lentiviral vector pWPI (Addgene plasmid 12254; constructed and submitted by Didier Trono). Lentiviral particles were produced by transfecting 293T cells with VSVG envelope plasmid, delta 8.9 gag/pol plasmid, and the plasmid of interest, as described previously (21), using Fugene (Roche) per the manufacturer's instructions. After 24 hours, the medium was changed to FGF/EGF neurosphere media, and supernatants were collected at 48 and 72 hours. These supernatants were pooled, passed through a 0.45-μm filter, and then frozen at −80°C until needed. Human neural stem and progenitor cells growing as neurospheres were triturated to small sphere size and then incubated with lentiviral supernatants in the presence of Polybrene for 24 hours. After approximately 1 week in culture, spheres could be identified, and they were then individually placed into wells of a 24-well plate. Spheres were visually scored for green fluorescent protein (GFP) positivity. Control cells were infected with pWPI empty vector, which constitutively expresses GFP. These cells were found to proliferate and behave identically to uninfected parental cells, and both parental and GFP cells were used as controls.

Establishment of pilocytic astrocytoma primary culture

Pilocytic astrocytoma primary cultures were established following the protocol previously described for primary glioblastoma cultures (22, 23). Freshly resected pilocytic astrocytoma tumors were placed into basal medium and dissected into 1-mm^3 sections. Tumor sections were then placed in papain solution (Sigma–Aldrich) and incubated at 37°C for 15 minutes. Dissociated tissue was passed through a Pasteur pipette several times, then centrifuged, and washed once with 10% serum-containing DMEM/Ham's F12 media. Cells were then plated in serum-containing DMEM/F12 media in tissue culture flasks.

Assays of cell proliferation, senescence, and telomere length

Bromodeoxyuridine (BrdU) assays were carried out as described previously (24). Cells were cytospun on to positively charged slides. After washing cells once with PBS, they were fixed with 4% paraformaldehyde for 15 minutes, permeabilized with 0.1% Triton/PBS, denatured with 0.1N HCl, washed in PBST (1× PBS Tween-20), and blocked with 5% normal goat serum/PBST or 5% BSA/PBST, and then incubated with the appropriate primary antibody. Anti-BrdU antibody was used as per the manufacturer's directions (Sigma B2531) at 1:100 dilution. After washing 3 times with PBST, cells were incubated for 45 minutes in the dark with the appropriate Cy-2- or Cy-3–conjugated secondary antibody (Jackson Immunoresearch). Cells were counterstained with 4′,6-diamidino-2-phenylindole (DAPI), mounted with antifade (Vectastain), and visualized by fluorescence microscopy.

DOI:10.1158/1078-0432.CCR-10-3349

Acidic β-galactosidase staining was done as per the manufacturer's instructions (Cell Signaling Technology kit #9860). Human neurosphere cells were plated on Matrigel-coated 24-well plates and incubated at 37°C for 48 hours to allow cells to extend processes before staining. Cells were then washed with PBS and fixed with a fixing solution. After 15 minutes, fixative was removed, and cells were washed twice with PBS and then incubated with staining solution. After staining, cells were washed with PBS and covered with 70% glycerol and photographed using a inverted light microscope. FISH of telomere length in GFP compared with $BRAF^{V600E}$-infected cells was carried out as previously described using cytospun cells (25).

Western blotting

Western blotting was carried out as described (24). Antibodies were used as per the manufacturer's instructions and were as follows: BRAF (Santa Cruz #SC-1660), $p16^{INK4a}$ (Santa Cruz #SC-56330), SOX2 (Santa Cruz #SC-17320), OLIG2 (Millipore AB9610), NESTIN (Millipore MAB 5326), glyceraldehyde-3-phosphate dehydrogenase (GAPDH; Research Diagnostics #10R-G109a), ERK (Cell Signaling Technologies #9102), and phospho-ERK (p-ERK; Cell Signaling Technologies #4376). Blots that have had intervening lanes removed are clearly marked with a white vertical line.

Colony formation in soft agarose

A 2× concentration of the neurosphere medium was prepared and mixed 1:1 with 1% melted agarose (Invitrogen) in water to make bottom agar, which was used to coat each well of a 6-well plate. Cells were incubated in Accutase (Sigma) and triturated by pipetting through a P1000 pipette to single cell density and placed into the top agarose/soft agarose mixture (0.5%) and immediately plated into 6-well plates at a density of 20,000 cells per well in 1.5 mL of agarose. After the agarose polymerized, 2 mL of the normal growth medium was placed into each well. Media were changed every 7 days, and the cultures were incubated for 4 to 6 weeks. Colonies were visualized by staining with 0.005% cresyl violet in PBS for 3 hours at room temperature. Colonies greater than 50 μm in diameter were scanned and counted using MCID Elite software.

Clinical specimens

Pilocytic astrocytoma and control tissues were obtained from the Johns Hopkins University School of Medicine Department of Pathology, with Institutional Review Board approval. All cases from 1990 to 2009 were reviewed to confirm the diagnosis of pilocytic astrocytoma and to determine whether sufficient material was still present in the paraffin block to be used in the construction of a tissue microarray. All cases that met these criteria (a total of 77) were included in the study. One older case (from 1988) and 2 pediatric infiltrating astrocytomas (grade 2) were included in the array to yield a total of 80 tumors, but the infiltrating astrocytomas were not included in the analyses described in this article. Tumor classification and cellularity were independently confirmed by 2 neuropathologists (D.J. and C.G.E.). No tumors were of the pilomyxoid variant. The tissue array was constructed as previously described (26), with 4 cores 0.6 mm in diameter taken from each tumor. Consistent with recently published reports, for purposes of data analysis, tumor location in the hypothalamus, optic chiasm, thalamus, and brainstem was designated as unfavorable whereas all other locations including cerebellum/posterior fossa, cerebral cortex, spinal cord, optic nerve, and fornix were considered favorable (27, 28). Of the 78 tumor samples, 66 were from primary tumor resections and had sufficient material to be scored for $p16^{INK4a}$ immunohistochemistry.

Immunohistochemistry

Sections from the pilocytic astrocytoma microarray were stained in the Johns Hopkins Hospital Pathology Department Central Laboratory according to standard clinical protocols using prediluted $p16^{INK4a}$ antibody (MTM Laboratories #CMA802) and p53 antibody (Ventana #760-2542; Roche). Only tumors with 2 or more evaluable cores were scored, and staining was classified using the following scale: strong (>50% of tumor cells showing immunoreactivity), moderate (between 10% and 50% of tumor cells showing immunoreactivity), weak (up to 10% of tumor cells showing immunoreactivity), and negative (no tumor cells showing immunoreactivity).

Statistical analysis

Statistical tests for laboratory experiments were carried out using GraphPad Prism (GraphPad Software) or Excel (Microsoft). All tests were 2-sided unless otherwise indicated, and P values less than 0.05 were considered significant. Error bars in all graphs represent SEM, unless otherwise indicated.

Stata 11 (StataCorp) was used for the descriptive and multivariate clinical analyses. Baseline characteristics of study patients and their tumors were evaluated according to $p16^{INK4a}$ expression status. P values were calculated with the use of Fisher's exact test for race, location, extent of resection, and therapy, the χ^2 test for sex, and the t test with unequal variance for age and follow-up time. Spearman's correlation tests were carried out to determine correlation between covariates.

An initial bivariate analysis with Fisher's exact test was carried out to estimate the association between $p16^{INK4a}$ expression status and mortality. Survival comparisons were made between $p16^{INK4a}$ negative cases and $p16^{INK4a}$ positive cases, with the latter defined as samples showing weak, moderate, or strong expression. We then conducted a survival analysis using the Kaplan–Meier estimator, and the log-rank test was used to compare survival distributions across groups. A univariate and multivariate Cox proportional hazards regression analysis was carried out with overall survival as the dependent variable. Risk factors

DOI:10.1158/1078-0432.CCR-10-3349

including age, sex, race, extent of resection, location of tumor, and therapy modality were considered for final model selection. The proportional hazards assumption was evaluated using complementary log–log plots and Schoenfeld residual plots.

Results

Expression of constitutively active BRAF^{V600E} activates the MAPK pathway in neural stem and progenitor cells and promotes soft agar colony formation

Normal neurospheres derived from developing human brain express markers for neural stem cells such as SOX2, OLIG2, and NESTIN and have the capability to differentiate into neurons, astrocytes, and oligodendroglia *in vitro* and *in vivo* (16, 17). To test the hypothesis that activation of BRAF would lead to transformation of human neural stem and progenitor cells, we infected neurospheres derived from human fetal cerebral cortex with a lentiviral construct containing constitutively active BRAF^{V600E}. Bulk cultures and subclones derived from single neurospheres including BRAF^{V600E} 1, 2, and 4 expressed high levels of BRAF as compared with controls (Fig. 1A). Cells transduced with BRAF^{V600E} also showed activation of downstream signaling, as evidenced by increased levels of p-ERK (Fig. 1A). These experiments were repeated with cortical neural stem cells isolated from an additional brain with similar results (Supplementary Fig. S1A).

Expression of BRAF^{V600E} did not lead to a dramatic increase in cell proliferation (Fig. 1B), with a nonsignificant 2% increase in the percentage of cells incorporating BrdU as compared with vector-infected controls (control = 11% BrdU positive, BRAF^{V600E} = 13% BrdU positive; $P = 0.33$, *t* test). To test the hypothesis that expression of constitutively active BRAF leads to the transformation of neural stem and progenitor cells, early-passage BRAF^{V600E}-transduced neurospheres were placed into soft agarose. After approximately 6 weeks in culture, BRAF^{V600E}-expressing cells formed a significantly larger number of colonies in soft agarose than in control cells (Fig. 1C and D; $P < 0.001$, *t* test). Interestingly, constitutively active BRAF was almost as effective in promoting growth in soft agar as the potent oncogenic combination of SV40 large T antigen and hTERT (Fig. 1D).

BRAF^{V600E} expression promotes senescence in human cortical neurospheres

Although their initial proliferation rate was equal to that of control cells, after approximately 5 passages in culture, the BRAF^{V600E}-transduced cells showed significantly decreased proliferation compared with controls (Fig. 2A and B; $P < 0.05$). Proliferation eventually completely ceased over the next few passages, though the cells appeared viable by light microscopy. In concert with this decreased growth, both the nuclear diameter and overall size of the cells growing in suspension increased, a change similar to the phenotype previously associated with oncogene-induced senescence (15). In contrast, at the point that the BRAF^{V600E}-expressing cells could no longer be passaged, GFP-transduced control cultures were still proliferating and had no change in their morphology (Fig. 2A; Supplementary Fig. S2).

To test the hypothesis that these cells had undergone oncogene-induced senescence, we conducted acidic β-galactosidase staining, which has been associated with the senescent phenotype in numerous studies (15, 29). We observed diffuse acidic β-galactosidase staining in BRAF^{V600E}-transduced cells, a 35-fold increase in percentage as compared with control cultures transduced with the same vector-only–expressing GFP (Fig. 2C and D). A human glioblastoma neurosphere culture (JHH-GBM10) grown in the same medium did not express acidic β-galactosidase (Fig. 2D), indicating that it was not a nonspecific effect of oncogenic transformation. To further confirm the induction of oncogene-induced senescence following BRAF activation, we analyzed 2 additional markers in protein lysates. Immunoblotting showed increased expression of the senescence-associated markers p16^{INK4a} (15) and PAI-1 (30) in BRAF^{V600E}-transduced cells as compared with controls (Fig. 2E; Supplementary Fig. S1B and C).

The passage number of the cultures used in these studies was below the threshold at which senescence due to telomere shortening generally occurs. However, to confirm that the senescent phenotype we observed was not due to effects on telomeres, we assessed their length by using FISH as previously described (25). This revealed similar telomere lengths (red fluorescence signal) between control proliferating GFP-expressing control cells and senescent BRAF^{V600E}-transduced cells, with no sign of overall shortening in either culture (Fig. 2F). A pancreatic carcinoma cell line (PANC), which is known to have shortened telomeres, exhibited reduced red fluorescence. Quantification of the telomere length showed that BRAF^{V600E}-transduced cells did not have shorter telomeres than GFP-transduced cells at the same passage number—in fact their telomeres were somewhat longer (Supplementary Fig. S3).

Lack of expression of the senescence marker p16^{INK4a} in pilocytic astrocytoma is associated with shorter survival

Examination of a tissue microarray containing 66 evaluable pilocytic astrocytomas showed that while 9 cases (14%) lacked p16^{INK4a} protein (Fig. 3A), the majority (86%) exhibited weak, moderate, or strong immunoreactivity for this senescence marker (Fig. 3B–D). Table 1 summarizes the characteristics of the 66 tumors with evaluable p16^{INK4a} staining. Most of the characteristics of the patients with p16^{INK4a}-negative tumors, including those commonly associated with outcome, were similar to those with p16^{INK4a}-positive tumors (location, time of follow-up, extent of resection, and need for additional therapy). There was a significant difference in the sex of the patients, with p16^{INK4a}-negative patients being more likely to be female than p16^{INK4a}-positive patients. There was a trend toward

DOI:10.1158/1078-0432.CCR-10-3349

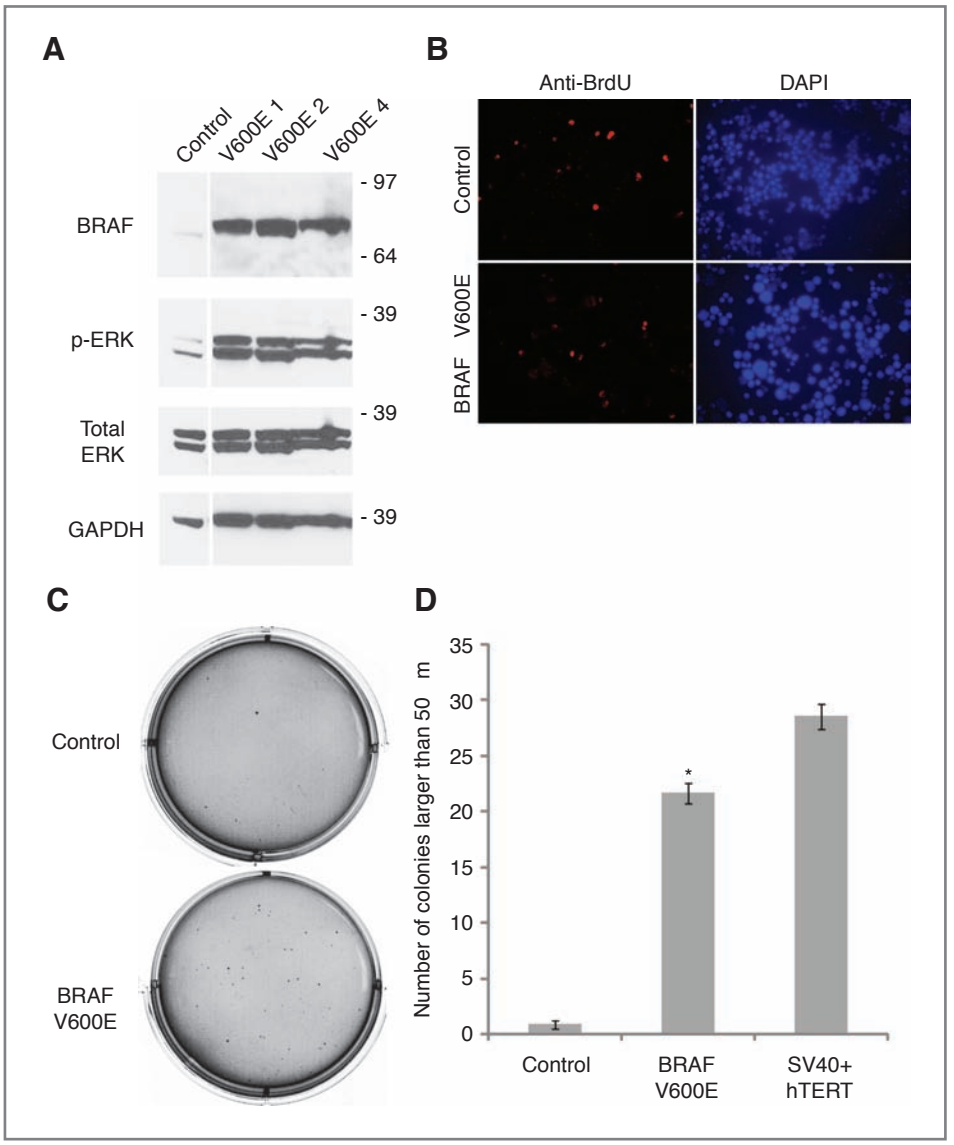

Figure 1. ERK activation, cellular proliferation, and colony formation in soft agarose following $BRAF^{V600E}$ transduction. A, Western blot showing that normal human neural stem and progenitor cells transduced with $BRAF^{V600E}$ lentivirus express higher levels of activated p-ERK than control neurospheres. V600E 1–4 represent separate subclones transduced with $BRAF^{V600E}$. B, proliferation as measured by BrdU incorporation is initially similar between control cells (top) and $BRAF^{V600E}$-infected cells (bottom), with 11% of control cells BrdU positive and 13% of $BRAF^{V600E}$ cells BrdU positive, $P = 0.33$, Student's t test. C, soft agarose experiment, showing that control cells (top) do not form large numbers of colonies compared with $BRAF^{V600E}$-transduced cells. D, quantification of soft agarose colony formation, including SV40 large T antigen and hTERT-transduced cells as positive controls. $BRAF^{V600E}$-infected cells show statistically significant increase in colony formation compared with control cortex neurosphere cells. *, $P < 0.0001$, control versus $BRAF^{V600E}$-infected cells, Student's t test.

increasing age in the $p16^{INK4a}$-negative patients, but this was not statistically significant.

Descriptive examination of characteristics of patients in this cohort regardless of $p16^{INK4a}$ staining showed positive Spearman's rank correlation coefficients between the extent of resection and the location of tumor (Spearman $\rho = 0.7$, $P < 0.001$), the extent of resection and therapy modality (Spearman $\rho = 0.59$, $P < 0.001$), and the location of tumor and therapy modality (Spearman $\rho = 0.41$, $P < 0.001$), indicating high correlation between these variables. These correlations are similar to those previously reported in low-grade gliomas (27, 28).

We also examined expression of TP53, another marker of senescence. TP53 staining was much less intense and was detected in only 18 of 78 (23%) pilocytic astrocytoma samples (Fig. 3E and F). However, TP53 immunoreactivity correlated significantly with that of $p16^{INK4a}$ in the 66 cases in which both could be scored (Spearman $\rho = 0.45$, $P = 0.0001$).

$p16^{INK4a}$ protein expression also correlated with outcome, with bivariate analysis revealing that 33% ($n = 3$) of $p16^{INK4a}$-negative patients died, compared with 3.6% ($n = 2$) of $p16^{INK4a}$-positive patients (Fisher's exact test, $P = 0.02$). Patients with tumors that were negative for $p16^{INK4a}$ also had significantly shorter overall survival when Kaplan–Meier survival curves were compared using the log-rank test ($P = 0.0002$; Fig. 3G). Univariate Cox proportional hazards regression analysis revealed that the relative risk of death was 13 times greater for patients with $p16^{INK4a}$-negative tumors than $p16^{INK4a}$-positive status (HR = 13.0, 95% CI: 2.1–80.5, $P = 0.006$). In multivariate analysis, we attempted to adjust for tumor location, type of resection, and therapy

DOI:10.1158/1078-0432.CCR-10-3349

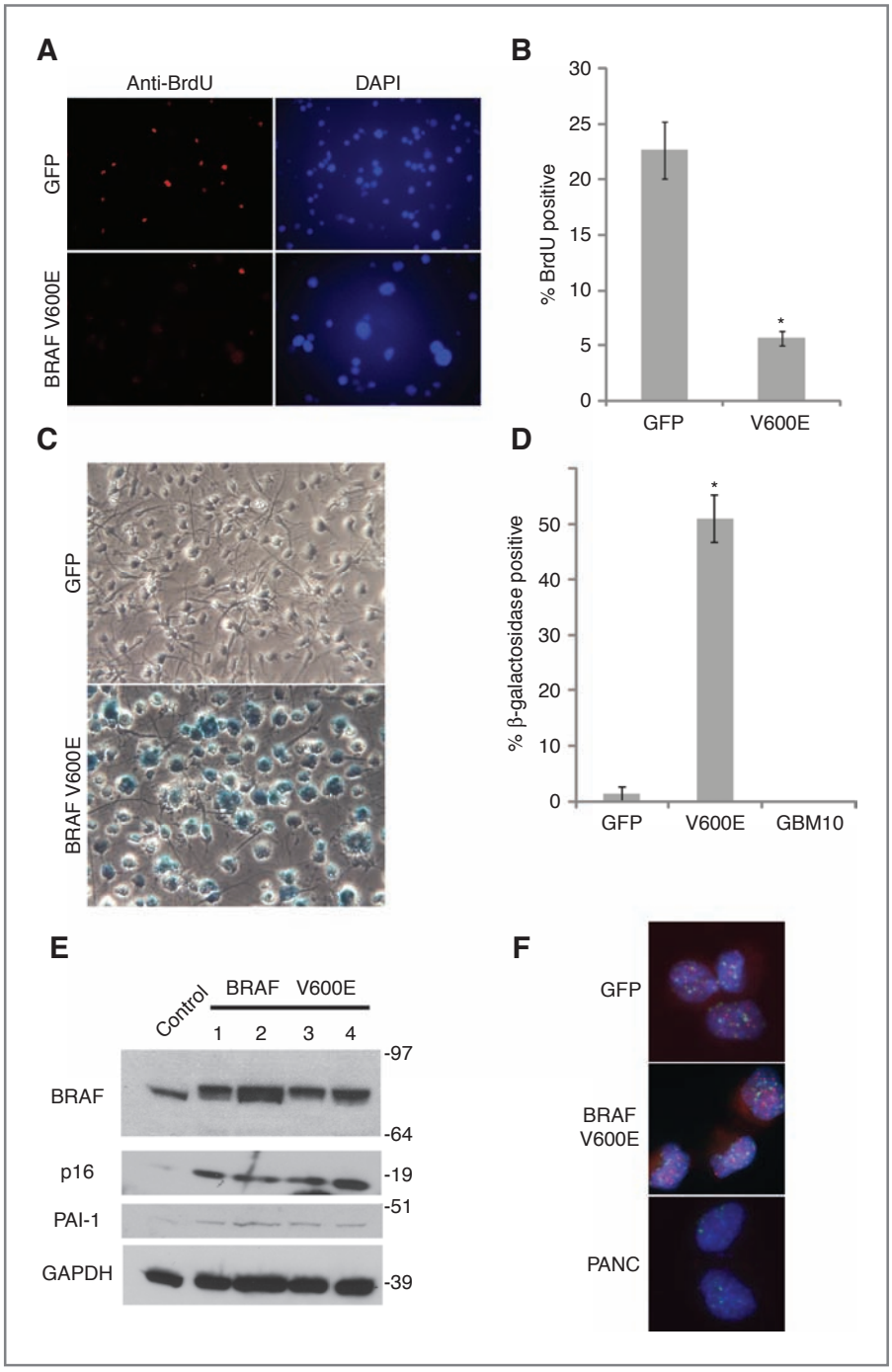

Figure 2. BRAF^{V600E}-expressing cells upregulate senescence markers and show decreased proliferation after several passages. A, immunofluorescence 200× photomicrographs of BrdU (red) and DAPI (blue)-stained GFP control and BRAF^{V600E}-expressing neural stem and progenitor cells. After 5 passages, BRAF^{V600E}-expressing neurosphere cells show increased nuclear size (DAPI) and decreased proliferation as measured by BrdU incorporation (bottom) compared with control neurospheres (top). B, quantification of BrdU positivity, showing percentage of BrdU-positive cells. *, $P < 0.05$, GFP versus BRAF^{V600E}-infected cells, Student's *t* test. C, bright field 200× photomicrographs of acidic β-galactosidase activity in control GFP and BRAF^{V600E}-infected neurosphere cells. Cells have been plated on an adherent substrate to allow for improved visualization of acidic β-galactosidase staining. Blue staining, indicating increased acidic β-galactosidase activity, is increased in BRAF^{V600E}-transduced cells, which also become enlarged when compared with GFP-expressing controls. D, quantification of acidic β-galactosidase activity, comparing the mean percentage of β-galactosidase–positive cells in GFP control and BRAF^{V600E}-transduced neural stem and progenitor cells. *, $P < 0.005$ GFP versus BRAF^{V600E}-infected cells, Student's *t* test. E, Western blotting showing increased p16^{INK4a} and PAI-1 expression in late-passage BRAF^{V600E}-expressing cells compared with controls. Senescent markers p16^{INK4a} and PAI-1 are induced in late-passage BRAF^{V600E}-expressing neurosphere cells compared with control neurosphere cells. BRAF^{V600E} 1–4 represent subclones isolated from the bulk infected culture. Molecular weight markers are located at the right of the blot. F, FISH analysis reveals similar telomere length in GFP control and BRAF^{V600E}-expressing neurosphere cells. Fluorescent 1000× photomicrographs of FISH-stained nuclei from similar passage GFP and BRAF^{V600E} neurospheres. At this passage, BRAF^{V600E}-transduced cells were highly senescent whereas GFP-expressing neurospheres continued to proliferate normally. Telomeres are labeled red, and centromeres are labeled green. Nuclei are counterstained with DAPI. PANC is a pancreatic carcinoma cell line with shortened telomeres and corresponding decreased red telomere signal.

DOI:10.1158/1078-0432.CCR-10-3349

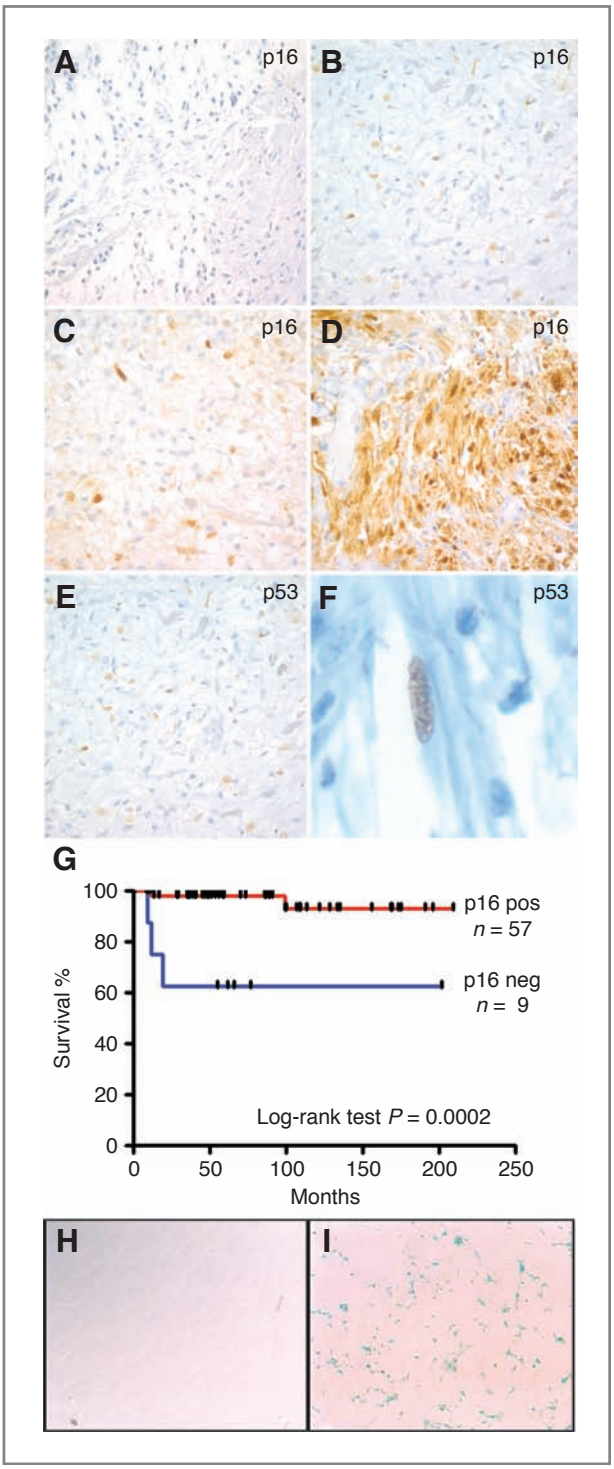

Figure 3. Pilocytic astrocytoma cells express markers of senescence *in vivo* and *in vitro*. Photomicrographs showing $p16^{INK4a}$ immunohistochemical staining in pilocytic astrocytoma specimens: negative (A); weak (B); moderate (C); and strong (D) $p16^{INK4a}$ immunohistochemical staining in pilocytic astrocytomas. E and F, immunohistochemical staining for p53 was largely negative, with only rare tumors showing scattered weakly staining cells. F, digitally expanded higher power view showing nuclear p53 staining in elongated tumor cell. (Original magnification 400× for A–F.) G, log-rank analysis of Kaplan–Meier curves showing significantly shorter overall survival in patients whose tumors were $p16^{INK4a}$ immunonegative ($P = 0.0002$). H and I, acidic β-galactosidase staining of an early-passage representative primary pilocytic astrocytoma culture. Bright field photomicrograph (100× power) showing prominent acidic β-galactosidase activity in primary pilocytic astrocytoma cells after 3 passages in culture (I), whereas human fibroblasts of equal density (H) do not stain after 10 passages.

modality, which were highly correlated, but comparison groups included only 0 or 1 death, so it was not possible to control for these predictors given the small sample size.

Primary cultures of KIAA1549:BRAF fusion-containing pilocytic astrocytoma express markers of senescence

To further determine whether pediatric pilocytic astrocytoma undergoes oncogene-induced senescence, we examined the senescence marker acidic β-galactosidase in low-passage primary pilocytic astrocytoma cultures established from freshly resected tumors. In 2 separate cultures that were derived from tumors harboring KIAA1549:BRAF fusions, we observed expression of the senescence marker in more than half of the cells at low passage. A representative image is shown in Figure 3I.

Induction of senescence is associated with downregulation of neural stem cell markers, including SOX2

The neural stem cell and somatic cell reprogramming factor *SOX2* is associated with the repression of $p16^{INK4a}$-mediated senescence in multiple cell systems (31, 32). To investigate the mechanism behind the induction of senescence in $BRAF^{V600E}$-transduced cells, we examined the expression of *SOX2* and other markers of neural stem cells in neurospheres that had undergone senescence. Compared with GFP-infected control cells, high expression of $BRAF^{V600E}$ led over time to decreased expression of the neural stem cell markers SOX2, OLIG2, and NESTIN (Fig. 4A). Expression of $p16^{INK4a}$ increased as neural stem cell marker expression decreased. The experiment was repeated in cortex-derived neurospheres from another brain, with similar loss of SOX2 expression in late passage neurospheres (Supplementary Fig. S1B and C). While $BRAF^{V600E}$-expressing neurospheres at early passage expressed SOX2 at levels comparable with GFP-infected controls (Supplementary Fig. S1B), after 5 passages, at the time when cells were exhibiting increased expression of senescent markers, the same $BRAF^{V600E}$ neurosphere subclone expressed less SOX2 than similar-passage GFP neurospheres (Supplementary Fig. S1C).

Discussion

Genetic alterations activating the RAS/RAF pathway, including $BRAF^{V600E}$, are a hallmark of pediatric pilocytic astrocytomas. We hypothesized that introducing $BRAF^{V600E}$ into human neural stem and progenitor cells would lead to cellular transformation similar to that seen in pilocytic astrocytoma or other pediatric gliomas. Interestingly,

DOI:10.1158/1078-0432.CCR-10-3349

Table 1. Characteristics of study patients and their tumors according to $p16^{INK4a}$ status

	Total	$p16^{INK4a}$ positive	$p16^{INK4a}$ negative	*P*
Patients in cohort	66	57	9	
Age, mean ± SD (range), y	14 ± 12 (0.5–52)	12 ± 10 (0.5–52)	25 ± 17 (9–51)	0.06
Sex				
Male	40 (60.6%)	38 (66.7%)	2 (22.2%)	0.01[a]
Female	26 (39.3%)	19 (33.3%)	7 (77.8%)	
Race				
White	55 (83.3%)	46 (80.7%)	9 (100%)	0.80
Black	7 (10.6%)	7 (12.3%)	0 (0%)	
Other	4 (6.1%)	4 (7%)	0 (0%)	
Follow-up, mean ± SD (range), mo	71 ± 55 (1–209)	73 ± 54 (1–209)	56 ± 62 (1–202)	0.40
Location[b]				
Favorable	40 (60.6%)	33 (57.9%)	7 (77.8%)	0.50
Unfavorable	26 (39.4%)	24 (42.1%)	2 (22.2%)	
Extent of resection				
Gross total	31 (47%)	26 (45.6%)	5 (55.6%)	0.70
Subtotal	35 (53%)	31 (54.3%)	4 (44.4%)	
Therapy[c]				
Initial surgery only	37 (56.1%)	32 (56.1%)	5 (55.6%)	1.0
Additional therapy	29 (43.9%)	25 (43.9%)	4 (44.4%)	
Radiation	18 (62.1%)	15 (60%)	3 (75%)	0.70
Repeat surgery	24 (82.8%)	21 (84%)	3 (75%)	1.0
Chemotherapy	7 (24.1%)	6 (24%)	1 (25%)	1.0
Outcome				
Alive	61 (92.4%)	55 (96.5%)	6 (66.7%)	0.02[a]
Died of disease	5 (7.6%)	2 (3.5%)	3 (33.3%)	

NOTE: *P* values were calculated using Fisher's exact test for race, location, extent of resection, therapy, and outcome; χ^2 test for sex; and *t* test with unequal variance for age and follow-up.

[a]Statistically significant value of $P < 0.05$.

[b]Unfavorable location was defined as a tumor located in the optic chiasm, thalamus, midbrain, or brain stem. All other locations were considered favorable.

[c]Patients receiving additional therapy may have received more than 1 modality. Percentages associated with each modality are of the total receiving additional therapy.

although there is no significant proliferative advantage to expression of $BRAF^{V600E}$ in these neurospheres, neural stem and progenitor cells did show increased colony formation in soft agar, indicating that expression of $BRAF^{V600E}$ was sufficient to promote some aspects of oncogenic transformation. This is similar to results previously reported for activating mutations in *BRAF* in nonstem cells (10). However, within several passages of BRAF activation, proliferation slowed in these cells, and they subsequently stopped growing entirely.

Activation of BRAF by V600E substitution is a hallmark not only of melanoma but also of benign melanocytic nevi. In the latter, oncogene-induced senescence is thought to limit the tumorgenicity of $BRAF^{V600E}$ (15). The cessation of proliferation of our $BRAF^{V600E}$-expressing cells in culture led us to investigate whether a similar cellular senescence phenotype might also operate in neural cells. $BRAF^{V600E}$-expressing human fetal cortical neurosphere cells show increased acidic β-galactosidase expression compared with controls and have increased expression of the senescence-associated markers PAI-1 and $p16^{INK4a}$. In primary human pilocytic astrocytomas, $p16^{INK4a}$ expression was identified using immunohistochemistry in 86% of the tumors on a tissue microarray containing 66 evaluable samples. Even in intensely stained tumors, there were piloid tumor cells without $p16^{INK4a}$ induction, suggesting that not all cells are uniformly senescent. This heterogeneity of $p16^{INK4a}$ expression may explain continued growth in a tumor that is also expressing markers of senescence.

CDKN2A locus deletion (encoding $p16^{INK4a}$ and $p19^{ARF}$) has been reported in pediatric low-grade astrocytoma and is associated with higher-grade pediatric gliomas (27, 33, 34). Deletion of the locus is often associated with expression of activating mutations in *BRAF* in these tumors. Recently, homozygous deletions

DOI:10.1158/1078-0432.CCR-10-3349

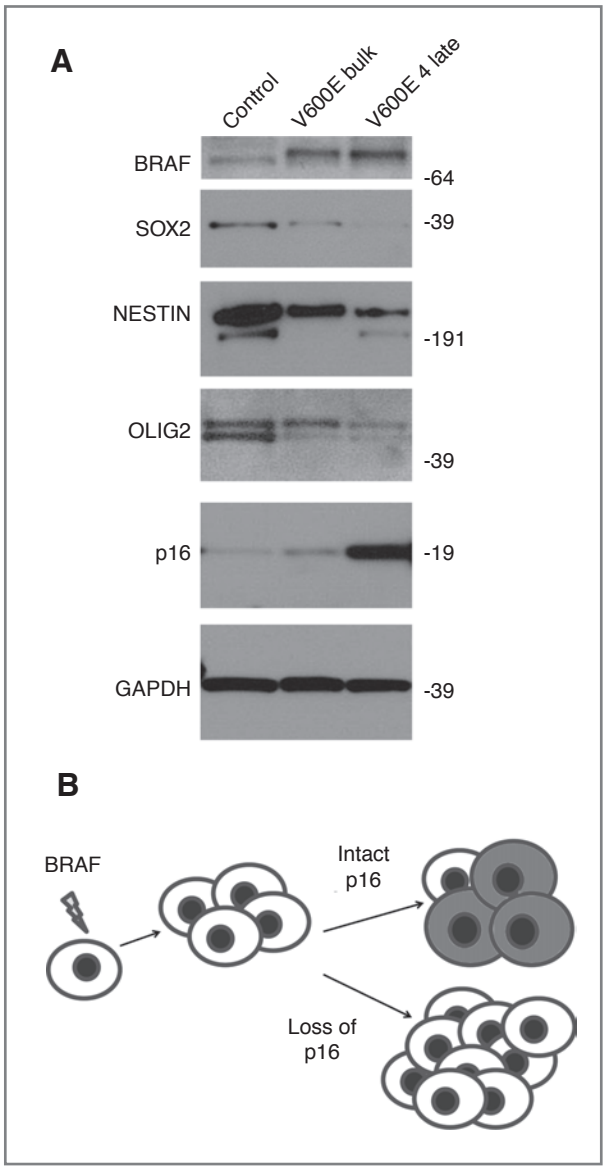

Figure 4. Onset of senescence in BRAF^{V600E}-expressing neurospheres corresponds to decreased expression of neural stem cell markers. A, Western blot showing decreased expression of neural stem cell markers in late-passage neurospheres (V600E 4) compared with the early-passage bulk culture infected with constitutively active BRAF. B, model for the formation of pilocytic astrocytoma. BRAF activation promotes initial transformation, but the induction of senescence (indicated by shaded cells) limits growth unless p16^{INK4a} is deleted or silenced.

affecting p16^{INK4a} were found selectively in more aggressive "anaplastic" pilocytic astrocytoma (33, 35). Consistent with this, we find that loss of p16^{INK4a} protein expression is associated in univariate analysis with worse outcomes in the pilocytic astrocytoma patients represented on our tissue microarray. This worse outcome could not be explained by location of the tumor, because unfavorable locations (e.g., hypothalamus optic chiasm/thalamus/brainstem) and subtotal resections were not overrepresented in the p16^{INK4a}-negative cohort (Table 1). A multivariate analysis was hampered by the relatively small size of our patient sample and the low number of deaths within the cohort. These data reveal the potential of p16^{INK4a} expression status as a predictor of survival, although future studies with greater numbers of patients are clearly needed to further explore this association. If validated in larger cohorts, p16^{INK4a} immunostaining may provide a tool for risk stratification in pilocytic astrocytoma. It also suggests that tumors in which cellular senescence does not occur (or tumors that escape from senescence) will behave in a more aggressive fashion.

Senescence due to telomere shortening has been investigated previously in pediatric low-grade gliomas (36). In our studies, we measured telomere length in senescent BRAF^{V600E}-expressing neurospheres and showed that they were longer than those of nonsenescent, control GFP neurospheres of the same passage number. In our model system, shortened telomeres do not account for the senescence phenotype, although it is possible that this plays a role *in vivo* in pilocytic astrocytoma.

Loss of stem cell markers in our system was also temporally associated with the induction of senescence. *SOX2* is a neural stem cell factor critical in somatic cell reprogramming and induced pluripotency. One of the functions of SOX2 is to suppress p16^{INK4a}-induced cellular senescence (31, 32). In our model system, we observe downregulation of SOX2 associated with the induction of senescence, consistent with this previously reported role. We also observe downregulation of other neural stem cell markers, such as OLIG2 and NESTIN, suggesting this phenomenon may not be causally related to *SOX2* but rather to depletion of stem cells in the culture.

In summary, we show that introduction of constitutively active BRAF^{V600E} into human cortical stem and progenitor cells initially promotes clonogenic growth in soft agar but ultimately results in dramatically reduced proliferation and arrested growth of the culture. Because this coincides with the induction of senescent markers, it strongly suggests that "oncogene-induced senescence" similar to that seen in melanocytic cells can occur in neural tissues, and this may explain the often indolent growth of pilocytic astrocytoma. Furthermore, examination of p16^{INK4a} expression in primary tumors suggests that escape from this process may underlie aggressive tumor growth. Further investigation of oncogene-induced senescence pathways may therefore provide new therapeutic opportunities in pilocytic astrocytoma.

Disclosure of Potential Conflicts of Interest

No potential conflicts of interest were disclosed.

Acknowledgments

We thank Donata Maciaczyk for her excellent technical support.

DOI:10.1158/1078-0432.CCR-10-3349

Grant Support

This study was supported by PLGA Foundation, Children's Cancer Foundation, Pilocytic/Pilomyxoid Astrocytoma Fund, and Lauren's First and Goal (C.G. Eberhart), St. Baldrick's Foundation Fellowship (E. H. Raabe), and Comprehensive Cancer Center Freiburg (J. Maciaczyk, U. Kahlert, and G. Nikkhah).

The costs of publication of this article were defrayed in part by the payment of page charges. This article must therefore be hereby marked *advertisement* in accordance with 18 U.S.C. Section 1734 solely to indicate this fact.

Received December 17, 2010; revised March 18, 2011; accepted April 5, 2011; published online June 2, 2011.

References

1. Pfister S, Witt O. Pediatric gliomas. Recent Results Cancer Res 2009;171:67–81.
2. Louis DN, Ohgaki H, Wiestler OD, Cavenee WK. WHO Classification of Tumours of the Central Nervous System. Lyon, France: IARC Press; 2007.
3. Gunny RS, Hayward RD, Phipps KP, Harding BN, Saunders DE. Spontaneous regression of residual low-grade cerebellar pilocytic astrocytomas in children. Pediatr Radiol 2005;35:1086–91.
4. Sievert AJ, Fisher MJ. Pediatric low-grade gliomas. J Child Neurol 2009;24:1397–408.
5. Sharma MK, Zehnbauer BA, Watson MA, Gutmann DH. RAS pathway activation and an oncogenic RAS mutation in sporadic pilocytic astrocytoma. Neurology 2005;65:1335–6.
6. Bar EE, Lin A, Tihan T, Burger PC, Eberhart CG. Frequent gains at chromosome 7q34 involving BRAF in pilocytic astrocytoma. J Neuropathol Exp Neurol 2008;67:878–87.
7. Jones DT, Kocialkowski S, Liu L, Pearson DM, Backlund LM, Ichimura K, et al. Tandem duplication producing a novel oncogenic BRAF fusion gene defines the majority of pilocytic astrocytomas. Cancer Res 2008;68:8673–7.
8. Pfister S, Janzarik WG, Remke M, Ernst A, Werft W, Becker N, et al. BRAF gene duplication constitutes a mechanism of MAPK pathway activation in low-grade astrocytomas. J Clin Invest 2008;118:1739–49.
9. Sievert AJ, Jackson EM, Gai X, Hakonarson H, Judkins AR, Resnick AC, et al. Duplication of 7q34 in pediatric low-grade astrocytomas detected by high-density single-nucleotide polymorphism-based genotype arrays results in a novel BRAF fusion gene. Brain Pathol 2009;19:449–58.
10. Jacob K, Albrecht S, Sollier C, Faury D, Sader E, Montpetit A, et al. Duplication of 7q34 is specific to juvenile pilocytic astrocytomas and a hallmark of cerebellar and optic pathway tumours. Br J Cancer 2009;101:722–33.
11. Janzarik WG, Kratz CP, Loges NT, Olbrich H, Klein C, Schafer T, et al. Further evidence for a somatic KRAS mutation in a pilocytic astrocytoma. Neuropediatrics 2007;38:61–3.
12. Forshew T, Tatevossian RG, Lawson AR, Ma J, Neale G, Ogunkolade BW, et al. Activation of the ERK/MAPK pathway: a signature genetic defect in posterior fossa pilocytic astrocytomas. J Pathol 2009;218:172–81.
13. Deshmukh H, Yeh TH, Yu J, Sharma MK, Perry A, Leonard JR, et al. High-resolution, dual-platform aCGH analysis reveals frequent HIPK2 amplification and increased expression in pilocytic astrocytomas. Oncogene 2008;27:4745–51.
14. Eisenhardt AE, Olbrich H, Roring M, Janzarik W, Van Anh TN, Cin H, et al. Functional characterization of a BRAF insertion mutant associated with pilocytic astrocytoma. Int J Cancer 2010 Dec 28. [Epub ahead of print].
15. Michaloglou C, Vredeveld LC, Soengas MS, Denoyelle C, Kuilman T, Van Der Horst CM, et al. BRAFE600-associated senescence-like cell cycle arrest of human naevi. Nature 2005;436:720–4.
16. Maciaczyk J, Singec I, Maciaczyk D, Klein A, Nikkhah G. Restricted spontaneous *in vitro* differentiation and region-specific migration of long-term expanded fetal human neural precursor cells after transplantation into the adult rat brain. Stem Cells Dev 2009;18:1043–58.
17. Maciaczyk J, Singec I, Maciaczyk D, Nikkhah G. Combined use of BDNF, ascorbic acid, low oxygen, and prolonged differentiation time generates tyrosine hydroxylase-expressing neurons after long-term *in vitro* expansion of human fetal midbrain precursor cells. Exp Neurol 2008;213:354–62.
18. Gilbertson RJ, Gutmann DH. Tumorigenesis in the brain: location, location, location. Cancer Res 2007;67:5579–82.
19. Braig M, Schmitt CA. Oncogene-induced senescence: putting the brakes on tumor development. Cancer Res 2006;66:2881–4.
20. Boehm JS, Zhao JJ, Yao J, Kim SY, Firestein R, Dunn IF, et al. Integrative genomic approaches identify IKBKE as a breast cancer oncogene. Cell 2007;129:1065–79.
21. Woods NB, Mikkola H, Nilsson E, Olsson K, Trono D, Karlsson S. Lentiviral-mediated gene transfer into haematopoietic stem cells. J Intern Med 2001;249:339–43.
22. Galli R, Binda E, Orfanelli U, Cipelletti B, Gritti A, De Vitis S, et al. Isolation and characterization of tumorigenic, stem-like neural precursors from human glioblastoma. Cancer Res 2004;64:7011–21.
23. Bar EE, Lin A, Mahairaki V, Matsui W, Eberhart CG. Hypoxia increases the expression of stem-cell markers and promotes clonogenicity in glioblastoma neurospheres. Am J Pathol 2010;177:1491–502.
24. Raabe EH, Laudenslager M, Winter C, Wasserman N, Cole K, LaQuaglia M, et al. Prevalence and functional consequence of PHOX2B mutations in neuroblastoma. Oncogene 2008;27:469–76.
25. Meeker AK, Hicks JL, Platz EA, March GE, Bennett CJ, Delannoy MJ, et al. Telomere shortening is an early somatic DNA alteration in human prostate tumorigenesis. Cancer Res 2002;62:6405–9.
26. Eberhart CG, Kratz J, Wang Y, Summers K, Stearns D, Cohen K, et al. Histopathological and molecular prognostic markers in medulloblastoma: c-myc, N-myc, TrkC, and anaplasia. J Neuropathol Exp Neurol 2004;63:441–9.
27. Horbinski C, Hamilton RL, Nikiforov Y, Pollack IF. Association of molecular alterations, including BRAF, with biology and outcome in pilocytic astrocytomas. Acta Neuropathol 2010;119:641–9.
28. Stokland T, Liu JF, Ironside JW, Ellison DW, Taylor R, Robinson KJ, et al. A multivariate analysis of factors determining tumor progression in childhood low-grade glioma: a population-based cohort study (CCLG CNS9702). Neuro Oncol 2010:12:1257–68.
29. Itahana K, Campisi J, Dimri GP. Methods to detect biomarkers of cellular senescence: the senescence-associated beta-galactosidase assay. Methods Mol Biol 2007;371:21–31.
30. Kortlever RM, Higgins PJ, Bernards R. Plasminogen activator inhibitor-1 is a critical downstream target of p53 in the induction of replicative senescence. Nat Cell Biol 2006;8:877–84.
31. Brazel CY, Limke TL, Osborne JK, Miura T, Cai J, Pevny L, et al. Sox2 expression defines a heterogeneous population of neurosphere-forming cells in the adult murine brain. Aging Cell 2005;4:197–207.
32. Basu-Roy U, Ambrosetti D, Favaro R, Nicolis SK, Mansukhani A, Basilico C. The transcription factor Sox2 is required for osteoblast self-renewal. Cell Death Differ 2010;17:1345–53.
33. Rodriguez EF, Scheithauer BW, Giannini C, Rynearson A, Cen L, Hoesley B, et al. PI3K/AKT pathway alterations are associated with clinically aggressive and histologically anaplastic subsets of pilocytic astrocytoma. Acta Neuropathol 2011;121:407–20.
34. Schiffman JD, Hodgson JG, VandenBerg SR, Flaherty P, Polley MY, Yu M, et al. Oncogenic BRAF mutation with CDKN2A inactivation is characteristic of a subset of pediatric malignant astrocytomas. Cancer Res 2010;70:512–9.
35. Rodriguez FJ, Scheithauer BW, Burger PC, Jenkins S, Giannini C. Anaplasia in pilocytic astrocytoma predicts aggressive behavior. Am J Surg Pathol 2010;34:147–60.
36. Tabori U, Vukovic B, Zielenska M, Hawkins C, Braude I, Rutka J, et al. The role of telomere maintenance in the spontaneous growth arrest of pediatric low-grade gliomas. Neoplasia 2006;8:136–42.